Available online at www.sciencedirect.com
SCIENCE DIRECT®
Journal of the European Ceramic Society 24 (2004) 3795–3800
www.elsevier.com/locate/jeurceramsoc

Intergranular film thickness of self-reinforced silicon carbide ceramics

Heon-Jin Choi [a,*], Young-Wook Kim [b]

[a] Department of Materials Science and Engineering, Korea Institute of Science and Technology, P.O. Box 131, Cheongryang, Seoul 130-650, South Korea
[b] Department of Materials Science and Engineering, University of Seoul, Seoul 130-743, South Korea

Received 1 July 2003; received in revised form 19 December 2003; accepted 27 December 2003

Available online 10 May 2004

Abstract

The intergranular film of self-reinforced SiC ceramics prepared by hot pressing and further annealing with SiO_2–Y_2O_3 and SiO_2–Al_2O_3 as sintering additives was observed by high-resolution transmission electron microscopy. The film thickness of SiC ceramics with SiO_2–Y_2O_3 was ~1.2 nm whereas that of ceramics with SiO_2–Al_2O_3 was ~0.8 nm. Based on the refined continuum model, an explanation on the variation of thickness with sintering additives is given. It seems that the behavior of intergranular glassy film of SiC ceramics is akin to that of Si_3N_4 ceramics.

Keywords: SiC; Liquid phase sintering; Electron microscopy; Grain boundaries; Interphase

1. Introduction

Many covalently bonded ceramics including SiC and Si_3N_4 are densified by liquid phase sintering using metal oxides as sintering additives. The oxides form a melt at relatively low temperature and remain at the grain boundaries as an intergranular glassy film (IGF) after sintering. Therefore, the existence of IGF is a common feature of these materials.[1–12] Recent studies have revealed that the thickness of IGF has a characteristic equilibrium value in the order of 0.5–2 nm, as observed by high-resolution transmission electron microscopy (HRTEM).[4–12]

The behavior of IGF in Si_3N_4 ceramics has been extensively studied by many investigators such as Kleebe,[13] Tanaka et al.,[4,14] Wang et al.,[15] and Burger et al.[16] These studies indicate that the behavior of IGF in Si_3N_4 ceramics is dominated by the composition of the sintering additives and the radius of cationic ions of sintering additives. Squeezing out IGF under moderate applied pressure (20–40 MPa) at some grain boundaries has also been observed. It has also revealed that the behavior of IGF is affected by the addition of anion (e.g., F).

Clarke[17] proposed a continuum model to explain the behavior of IGF based on an attractive van der Waals and a repulsive steric force. The attractive force originates from the electromagnetic interaction between fluctuating dipoles in the different phases (i.e., grain and IGF). The origin of the repulsive force is the structure of IGF that resists disordering. This model successfully predicts that the IGF has an "equilibrium thickness" in the order of several nanometers. However, the model could not explain the effect of sintering additives on the behavior of IGF since it assumes that the IGF is a pure SiO_2 phase.[17] The important consequence of this assumption is that only the structural properties (i.e., correlation length) of the IGF can be considered to evaluate the effect of sintering additives on the behavior of IGF. However, the physical properties as well as the structural properties of the IGF by the incorporation of cations or anions in the sintering additives affect on the behavior of IGF.

In the previous study, we refined the continuum model based on the bond strength between cation and anion in the IGF since it controls the electromagnetic interaction of fluctuating dipoles in the IGF and the force to resist disordering of the glass phase.[18] The refined model indicates that both the attractive van der Waals and repulsive steric forces will be changed with the incorporation of additive ions in the IGF. Moreover, the charge, size and amount of ions are important to the force balance and behavior of the IGF. The refined model successfully explained the variation of IGF thickness of Si_3N_4 ceramics doped with different sintering additives and the squeezing out of IGF from some grain

* Corresponding author. Fax: +82-2-958-5509.
E-mail address: hjchoi@kist.re.kr (H.-J. Choi).

0955-2219/$ – see front matter © 2004 Elsevier Ltd. All rights reserved.
doi:10.1016/j.jeurceramsoc.2003.12.029

boundaries in hot-pressed Si_3N_4 ceramics under moderate external pressure (e.g., 25 MPa).

As compare to Si_3N_4 ceramics, the behavior of the IGF in liquid-phase sintered-, self-reinforced SiC ceramics has not been studied in detail. Considering the potential of self-reinforced SiC ceramics as room- and high-temperature structural materials, the understanding of the origin and behavior of IGF is important to improve their properties in applications. In this study, we prepared self-reinforced SiC ceramics with SiO_2–Y_2O_3, and SiO_2–Al_2O_3 as sintering additives, observed the thickness of IGF, and discussed the variation of thickness of IGF based on the refined continuum model. Since the continuum model deals with equilibrium intergranular states of ceramics, we only analyzed densified and further heat-treated SiC ceramics that have equilibrium microstructures for a given system. Limited experimental evidence for the change of IGF thickness in SiC ceramics is coincident with the calculation of equilibrium thickness of IGF by the refined continuum model. Though the IGF behavior of SiC ceramics can be more accurately addressed by further considering other factors contribution such as the liquid phase composition and/or annealing effects, our preliminary result indicate that the behavior of IGF with sintering additives in liquid-phase sintered SiC ceramics is akin to that of liquid-phase sintered Si_3N_4 ceramics.

2. Experimental procedure

α-SiC (A-1 grade, Showa Denko, Tokyo, Japan), SiO_2, Y_2O_3 (99.9% pure, Shin-Etsu Chemical Co., Tokyo, Japan), and Al_2O_3 (AKP 30, Sumitomo Co., Tokyo, Japan) were used as the starting powders. The mean particle size and the specific surface area of the α-SiC powders were 0.45 μm and 15 m^2/g, respectively.

Two batches of powder were mixed: one batch containing 88 wt.% SiC, 7.8 wt.% Y_2O_3, and 4.2 wt.% SiO_2 (composition corresponding to SiC–$Y_2Si_2O_7$ tie-line, denoted as SCY) and the other batch containing 88 wt.% SiC, 7.8 wt.% Al_2O_3, and 4.2 wt.% SiO_2 (denoted as SCA). Individual batches were milled in ethanol for 24 h using SiC grinding balls. The milled slurry was dried, sieved, and hot-pressed at 1850 °C for 1 h under a pressure of 25 MPa in Ar atmosphere. The hot-pressed materials were further annealed at 1950 °C for 1 h under an atmospheric pressure of Ar.

The hot-pressed and annealed samples were cut, polished, and then etched by a plasma of CF_4 containing 7.8% O_2. The microstructures were observed by scanning electron microscopy (SEM). Thin foils for high-resolution transmission electron microscopy (HRTEM, Philips CM30, Eindhoven, The Netherlands) were prepared by the standard procedures of grinding, dimpling, and argon-ion-beam thinning followed by carbon coating to minimize charging during observation.

3. Results and discussion

The hot-pressed and annealed SCY and SCA showed 97.2 and 95.7% of relative densities. Typical microstructures for SCY and SCA before- and after-annealing are shown in Fig. 1. Both the as hot-pressed materials show the microstructure consisted of equiaxed grains with similar grain size. However, SCA showed large grain growth with elongated grains during annealing whereas SCY showed a little grain growth with equiaxed grains. Faster growth rate of SiC in SCA may be due to lower viscosity of Al_2O_3–SiO_2 liquid at the annealing temperature. Al_2O_3–SiO_2 system forms a liquid at 1595 °C whereas Y_2O_3–SiO_2 system forms a liquid at 1660 °C. Furthermore, Al^{3+} can substitute Si^{4+} in $SiO_4{}^{4-}$ network structure and seriously lower the viscosity of IGF at high temperature. However, Y^{3+} cannot substitute Si in the network structure, therefore, it does not lower the viscosity of IGF seriously like Al^{3+}.[18,19] Further annealing longer than 1 h did not change the macrostructures. Thus, the microstructure obtained in this study could be an equilibrium microstructure for each given system and, thus, suitable to address the equilibrium IGF behavior of SiC ceramics. Since the continuum model deals with equilibrium intergranular states of ceramics, we only analyzed densified and further heat-treated SiC ceramics.

Fig. 2 shows typical IGF of SCY and SCA observed by HRTEM. The thicknesses of IGF of SCY and SCA are about 1.2 and 0.8 nm, respectively. Although the limited number of grain boundaries have been observed in this study (three grain boundaries in each materials), it is believed that the thickness of IGF in SCY is wider than that of SCA.

According to the continuum model, the force balance in IGF can be expressed as:[17]

$$\prod_{\text{disp}} + \prod_{\text{st}} + \sigma = 0 \tag{1}$$

where $\prod_{\text{disp}}$ is the attractive van der Waals force, $\prod_{\text{st}}$ is the repulsive steric force and σ is the local compressive stress. $\prod_{\text{disp}}$ and $\prod_{\text{st}}$ are expressed as:

$$\prod_{\text{disp}} = \frac{H_{\beta g \beta}}{6\pi h^3} \tag{2}$$

and

$$\prod_{\text{st}} = -4a\eta_0^2 \exp\left(-\frac{h}{\xi}\right) \tag{3}$$

where $H_{\beta g \beta}$ is the Hamaker constant, the subscript β and g denotes the matrix (i.e., grain) and the IGF, respectively, h is the IGF thickness, $a\eta_0^2$ corresponds to the free energy difference between IGF liquids with and without structural ordering, η_0 is the degree of epitaxy, a corresponds to the heat of melting, and ξ is the structural correlation length. In

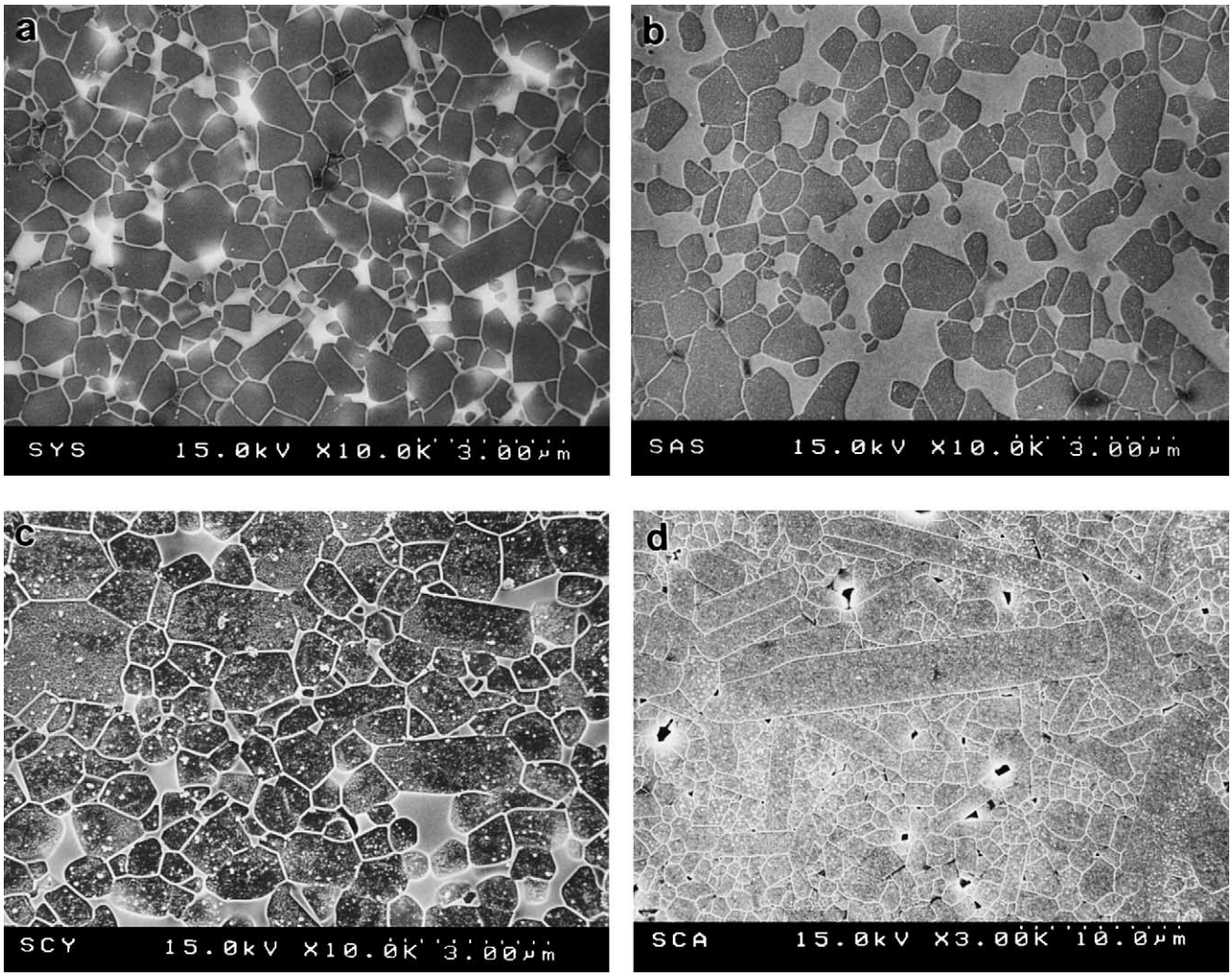

Fig. 1. Microstructures of (a) as-hot-pressed SCY, (b) as-hot-pressed SCA, (c) hot pressed and annealed SCY, and (d) hot pressed and annealed SCA.

Eq. (2), the $\prod_{\text{disp}}$ can be calculated from the approximation of the $H_{\beta g \beta}$, which is expressed as:

$$H_{\beta g \beta} = \frac{3}{4} kT \left(\frac{\varepsilon_\beta - \varepsilon_g}{\varepsilon_\beta + \varepsilon_g} \right)^2 + \frac{3\pi\eta\nu_e}{8\sqrt{2}} \frac{(n_\beta^2 - n_g^2)^2}{(n_\beta^2 + n_g^2)^{3/2}} \quad (4)$$

where kT is the Boltzmann constant times the absolute temperature, ε and n are the low-frequency dielectric constant and refractive index, respectively, η is the Planck's constant divided by 2π, and ν_e is the absorption frequency.

By using Eqs. (1)–(4), one can calculate the thickness of IGF. However, the change of attractive and repulsive force of IGF with physical properties of IGF (i.e., dielectric constant and refractive index for Hamaker constant, and heat of melting for steric force), due to the incorporation of cation of sintering additives to IGF, cannot be addressed in this calculation.

The refined continuum model estimates the effect of sintering additives by introducing field strength between cation and anion in the IGF since it dominates the physical properties of IGF and, in turn, the behavior of IGF.[18] According to the refined model, the dielectric constant and refractive index of IGF, which determine the Hamaker constant and attractive force of IGF, can be estimated as follows:

$$\varepsilon_{SiO_2\text{-Rc}} = \frac{\varepsilon_{SiO_2}}{(1 - x + xF_R)} \quad (5)$$

where $\varepsilon_{SiO_2\text{-Rc}}$ and ε_{SiO_2} are the dielectric constants of the IGF with Rc-containing SiO_2 glass and the IGF with pure SiO_2 glass, respectively. Rc indicates the cation of sintering additives incorporated in the IGF. F_R is the relative field strength which can be expressed as follows:

$$F_R = \frac{F_{\text{Rc-O}}}{F_{\text{Si-O}}} = \frac{(R_{Si} + R_O)^2 Z_{Rc}}{(R_{Rc} + R_O)^2 Z_{Si}} \quad (6)$$

where R_{Si}, R_{Rc} and R_O are the ionic radii of Si, Rc, and O ions, respectively, and Z_{Si} and Z_{Rc} are the charge of Si and Rc ions, respectively. In a same procedure, the refractive index could be given as follows:

$$n_{SiO_2\text{-Rc}} = \frac{n_{SiO_2}}{(1 - x + xF_R)} \quad (7)$$

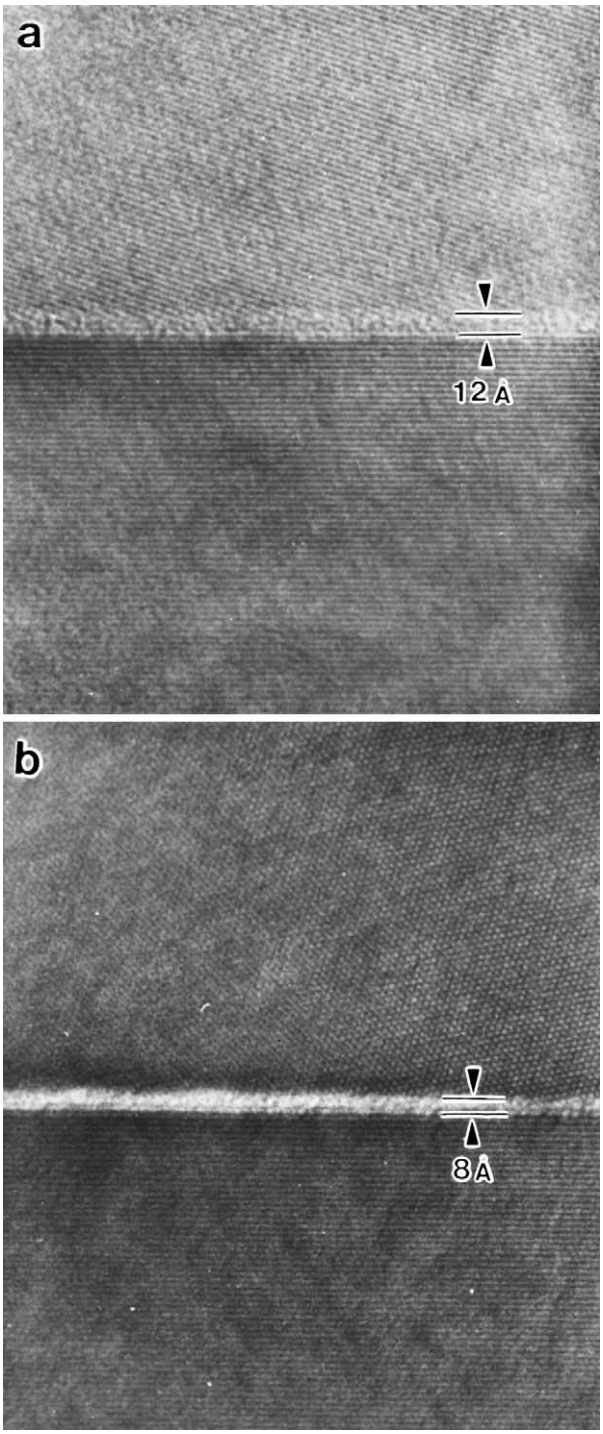

Fig. 2. Representative HRTEM micrographs of grain boundaries in hot-pressed and further annealed SiC ceramics: (a) a glass film in the boundary in SCY; and (b) a glass film in the boundary in SCA.

where $n_{SiO_2\text{-Rc}}$ and n_{SiO_2} are the refractive indices of the IGF with Rc-containing SiO_2 glass and the IGF with pure SiO_2 glass, respectively. By using Eqs. (2), (4)–(7), one can calculate the attractive force of IGF with consideration of the effect of sintering additives. Supposing that the repulsive steric force to the disordering of glass phase is proportional to the field strength of the bond, the repulsive steric force of IGF with Rc-containing SiO_2 glass can be estimated by introducing F_R in Eq. (3) as follows:

$$\prod_{st_{SiO_2\text{-Rc}}} = \prod_{st_{SiO_2}} F_R = -4F_R a_{SiO_2} \eta_0^2 \exp\left(-\frac{h}{\xi_{SiO_2}}\right) \quad (8)$$

where a_{SiO_2} and ξ_{SiO_2} are the heat of melting and structural correlation length of the pure SiO_2 glass, respectively. Then, by using Eqs. (1)–(8), one can calculate the thickness of IGF with consideration of the effect of sintering additives on the physical properties of IGF.

Fig. 3a shows the calculated equilibrium thickness of IGF in SiC ceramics with sintering additives (i.e., SCY and SCA) by using the refined continuum model. For the calculation, it is assumed that the correlation length, ξ, is constant as 0.3 nm;[17] the fraction of Y–O or Al–O bonds in the total bonds, x, of the IGF is 0.36;[20] the dielectric constant and refractive index of SiC are 10.20[17] and 2.65,[17] respectively; and $\sigma = 0$ since both materials were annealed at 1950 °C without applied pressure. Fig. 3a indicates that the addition of Y_2O_3 or Al_2O_3 increases the thickness of IGF. It also indicates that the thickness of IGF will be wider in SCY as compare to SCA. This is due to the decrease in the attractive force with larger cationic radius of Y^{3+} (0.090 nm) as compared to Al^{3+} (0.039 nm). Both the attractive and repulsive forces are decreased with increasing cationic radius by changing the physical constants, ε, n, and a of IGF, but the attractive force is more affected.

Fig. 3b shows the calculated equilibrium thickness of IGF in SiC ceramics with sintering additives by using the previous continuum model. In this calculation, it is assumed that all the constants, ε, n, and a are constant corresponding to the value of pure SiO_2 phase, except the correlation length, ξ. The correlation length assumed to be affected by the incorporation of sintering additives to IGF. By assuming that SiO_2 glass phase follows the hard sphere model and x is 0.36, the correlation length of IGF in SCY and SCA are roughly estimated as 0.552 and 0.348, respectively. For example, correlation length of IGF in SCY is estimated as follows; $\xi_{SCY} = \xi_{SiO_2}(1-x) + \xi_{SiO_2} x R_Y / R_{Si}$, where ξ_{SCY} is the correlation length of IGF with Y-containing SiO_2 glass, ξ_{SiO_2} is the correlation length of the IGF with pure SiO_2 glass (~0.3 nm), R_Y and R_{Si} are the ionic radii of Y^{3+} and Si^{4+}, respectively. Fig. 3b also indicates that the addition of Y_2O_3 or Al_2O_3 increases the thickness of IGF, and the thickness of IGF in SCY will be wider than that of SCA. However, such a large increment of the IGF thickness as shown in Fig. 3b with the addition of Y_2O_3 or Al_2O_3 could not be expected in the observation of IGF in SiC ceramics. Although the estimation of correlation length in this study remains a question, the thickness variation of IGF for SCY and SCA may be reasonably explained by the change of physical properties of IGF with sintering additives rather than the change of structural properties of IGF since the calculation of the thickness based on the refined continuum

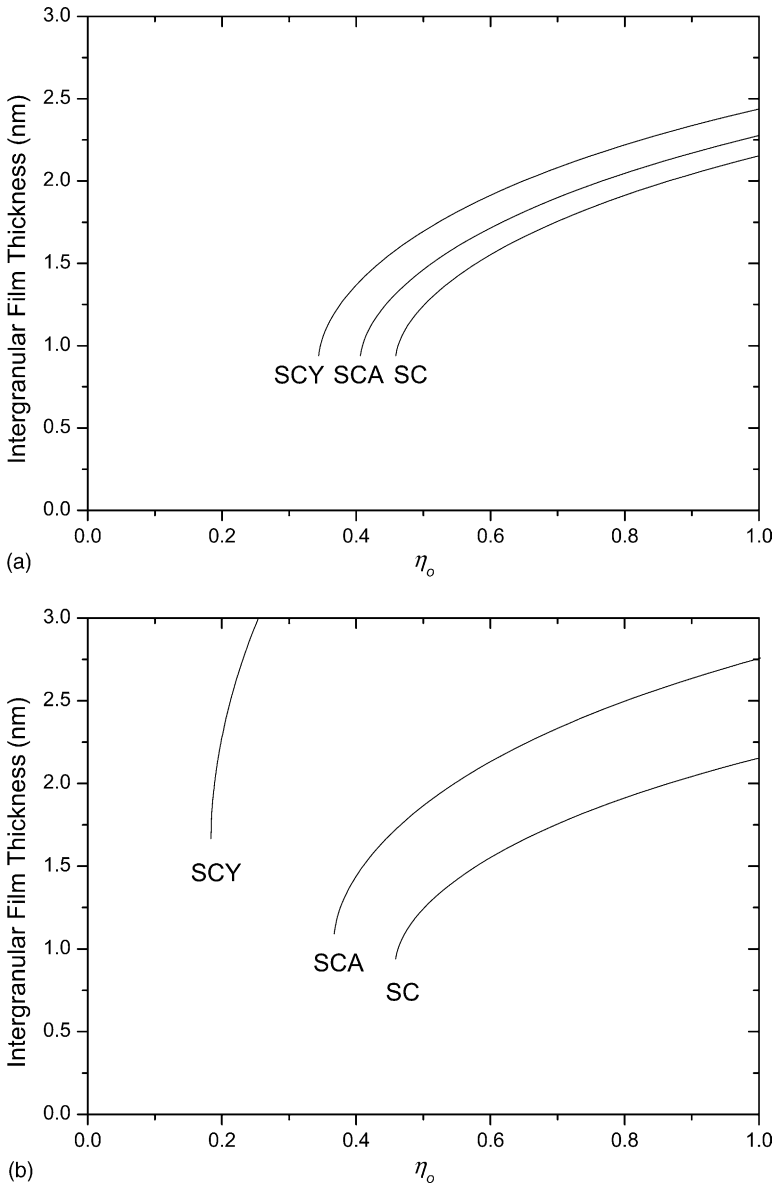

Fig. 3. Calculated equilibrium thickness of intergranular film in SiC ceramics: (a) based on the refined continuum model; and (b) based on the continuum model. SC indicates the equilibrium thickness of intergranular film in SiC ceramics by assuming that the film is a pure SiO_2 phase.

model shows the more consistency with the experimental evidence.

It is noted that the increases in IGF thickness with cationic radius of sintering additives for SiC ceramics has also been reported in Si_3N_4 ceramics.[8,18] It implies that the effect of sintering additives on the behavior of IGF may have a similar trends with that of Si_3N_4 ceramics and, therefore, the general rule for the selection of sintering additives for Si_3N_4 ceramics may also be true for SiC ceramics.

Finally, it should stressed that the IGF behavior of SiC ceramics can be more precisely addressed by further considering other factors contribution such as the liquid phase composition and/or annealing effects. Our results presented here mainly illustrate the effect of cationic radius, however, could be used as starting point for further investigation. Thus, it may helpful to understand the effect of other parameters as well as cationic radius on the behavior of IGF in SiC ceramics.

4. Summary

The self-reinforced SiC ceramics were prepared by hot-pressing and further annealing with Y_2O_3–SiO_2 and Al_2O_3–SiO_2 as sintering additives, and the intergranular glassy films were observed by high-resolution electron microscopy. It seems that the thickness of intergranular

glassy film of SiC ceramics increases with the cationic radius of sintering additives, akin to that of Si_3N_4 ceramics. The refined continuum model explains the behavior of intergranular film reasonably.

References

1. Clarke, D. R. and Thomas, G., Grain boundary phase in a hot-pressed MgO fluxed silicon nitride. *J. Am. Ceram. Soc.* 1977, **60**(11/12), 491–495.
2. Lou, L. K. V., Mitchell, T. E. and Heuer, A. H., Impurity phases in hot-pressed Si_3N_4. *J. Am. Ceram. Soc.* 1978, **61**(9/10), 392–396.
3. Krivanek, O. L., Shaw, T. M. and Thomas, G., The microstructure and distribution of impurities in hot-pressed and sintered silicon nitrides. *J. Am. Ceram. Soc.* 1979, **62**(11/12), 585–590.
4. Tanaka, I., Kleebe, H.-J., Cinibulk, M. K., Bruley, J., Clarke, D. R. and Rühle, M., Calcium concentration dependence of the intergranular film thickness in silicon nitride. *J. Am. Ceram. Soc.* 1994, **77**(4), 911–914.
5. Cinibulk, M. K., Kleebe, H.-J., Schneider, G. A. and Rühle, M., Amorphous intergranular films in silicon nitride ceramics quenched from high temperature. *J. Am. Ceram. Soc.* 1993, **76**(11), 2801–2808.
6. Verantano, J. S., Kleebe, H.-J., Hampp, E., Hoffman, M. J. and Rühle, M., Yb_2O_3-fluxed sintered silicon nitride. *J. Mater. Sci.* 1993, **28**, 3529–3538.
7. Kleebe, H.-J., Braue, W., Schmidt, H., Pezzotti, G. and Ziegler, G., Transmission electron microscopy of microstructures in ceramic materials. *J. Eur. Ceram. Soc.* 1996, **16**, 339–351.
8. Wang, C. M., Pan, X., Hoffman, M. J., Cannon, R. M. and Rühle, M., Grain boundary films in rare-earth-glass-based silicon nitride. *J. Am. Ceram. Soc.* 1996, **79**(3), 788–792.
9. Pan, X., Gu, H., Weeren, R., Danforth, S. C., Cannon, R. M. and Rühle, M., Grain-boundary microstructure and chemistry of a hot isostatically pressed high-purity silicon nitride. *J. Am. Ceram. Soc.* 1996, **79**(9), 2313–2320.
10. Wang, H. and Chiang, Y.-M., Thermodynamic stability of intergranular amorphous films in bismuth-doped zinc oxide. *J. Am. Ceram. Soc.* 1998, **81**(1), 89–96.
11. Kim, Y.-W., Mitomo, M. and Nishimura, T., Hear-resistant silicon carbide with AlN and Er_2O_3. *J. Am. Ceram. Soc.* 2001, **84**(9), 2060–2064.
12. Kim, Y.-W., Mitomo, M. and Zhan, G.-D., unpublished work.
13. Kleebe, H.-J., Structure and chemistry of interfaces in Si_3N_4 ceramics studied by transmission electron microscopy. *J. Ceram. Soc. Jpn.* 1997, **105**(6), 453–475.
14. Tanaka, I., Igashira, K., Kleebe, H.-J. and Rühle, M., High-temperature strength of fluorine-doped silicon nitride. *J. Am. Ceram. Soc.* 1994, **77**(1), 275–277.
15. Wang, C. M., Mitomo, M., Nishimura, T. and Bando, Y., Grain boundary film thickness in superplastically deformed silicon nitride. *J. Am. Ceram. Soc.* 1997, **80**(5), 1213–1221.
16. Burger, P., Duclos, R. and Crampon, J., Microstructure characterization in superplastically deformed silicon nitride. *J. Am. Ceram. Soc.* 1997, **80**(4), 879–885.
17. Clarke, D. R., On the equilibrium thickness of intergranular glass phases in ceramic materials. *J. Am. Ceram. Soc.* 1987, **70**(1), 15–22.
18. Choi, H. J., Kim, G. H., Lee, J. G. and Kim, Y.-W., Refined continuum model on the behavior of intergranular film in silicon nitride ceramics. *J. Am. Ceram. Soc.* 2000, **83**(11), 2821–2827.
19. Choi, H. J., Lee, J. G. and Kim, Y.-W., Oxidation behavior of liquid phase sintered silicon carbide ceramics with AlN and Re_2O_3 (Re = Y, Er, Yb). *J. Am. Ceram. Soc.* 2002, **85**(9), 2281–2286.
20. Ohashi, M., Nakamura, K., Hirao, K., Kanzaki, S. and Hampshire, S., Formation and properties of Ln–Si–O–N glasses (Ln = Lanthanides or Y). *J. Am. Ceram. Soc.* 1995, **78**(1), 71–76.